

# Identifying Damage Types in Solar Panels Through Surface Image Analysis with Naive Bayes

Ninuk Wiliani<sup>1</sup>(✉), Titik Khawa<sup>1,2</sup>, Suzaimah Ramli<sup>2</sup>

<sup>1</sup> Pancasila University, Jakarta, Indonesia

<sup>2</sup> Asia e University, Kuala Lumpur, Malaysia

ninuk.wiliani@univpancasila.ac.id

---

## Article Info

### Article history:

Received December 12, 2024

Revised December 21, 2024

Accepted December 21, 2024

---

### Keywords:

Solar Panel Defect Classification

Statistical Feature Extraction

Naive Bayes Algorithms

Digital Image Analysis

Performance Evaluation Metrics

---

## ABSTRACT (10 PT)

The growing utilization of solar panels as a renewable energy source requires efficient maintenance solutions to guarantee their best functioning. Identifying and categorizing faults on solar panel surfaces is essential for maintenance, as these defects considerably affect energy output and system efficiency. This study investigates the utilization of statistical feature extraction methods alongside Bernoulli Naive Bayes (BNB) and Gaussian Naive Bayes (GNB) algorithms to categorize different defect types, such as cracks, scratches, spots, and non-defective surfaces, through digital image analysis. Statistical criteria, including recall, specificity, and area under the curve (AUC), are employed to assess model performance. The findings indicate that the GNB algorithm surpasses BNB, with a mean average precision (mAP) of 39.83% with an 85:15 training-test ratio, whereas BNB reaches a maximum mAP of 29.25% at a 90:10 ratio. Nonetheless, both models demonstrate constraints in precision, as indicated by a total AUC of 0.644. This work illustrates the potential of statistical feature extraction approaches for defect classification, while emphasizing the necessity for future improvements to boost the efficacy of feature extraction and classification techniques in practical applications.

*This is an open access article under the [CC BY-SA](#) license.*



---

## Corresponding Author:

Ninuk Wiliani

Pancasila University, Jakarta, Indonesia

Email: ninuk.wiliani@univpancasila.ac.id

---

## 1. INTRODUCTION

In recent years, the use of renewable energy sources, particularly solar energy, has become more popular as a substitute for energy sources that are environmentally friendly and dependable[1]. Solar panels play a significant role in the process of converting sunlight into clean electrical energy[2]. However, solar panels often experience various [3], such as cracks, scratches, and stains, caused by exposure to extreme weather, dust, and other environmental factors. This damage can reduce the effectiveness of sunlight absorption, which in turn decreases the electrical power generated by the solar panels[4]. This condition implies a decrease in energy efficiency, as well as contributing to increased maintenance costs and reduced panel lifespan. With the increasing use of solar panels in various sectors, the need to detect and classify surface damage on the panels with high accuracy and efficiency is becoming more urgent[5]. Early detection of panel damage allows for timely maintenance or replacement, thereby contributing to the maintenance of optimal performance and maximizing the lifespan of the panels. Methods that can be applied to identify damage on solar panels involve texture feature extraction using a statistical approach[6]. This method allows for the identification of specific texture patterns that may indicate the type of damage on the panel surface.

This research focuses on the significance of early detection of damage occurring on the surface of solar panels. Solar panels often face several damages, including cracks, scratches, and stains caused by environmental exposure and extreme weather conditions[7]. This damage has the potential to reduce the efficiency of solar panels in generating energy and can lead to increased maintenance costs if not identified early on. The texture-based feature extraction method using statistical indicators such as Mean, Variance, Standard Deviation, Skewness, Kurtosis, and Entropy is expected to identify various types of damage on the panel surface with a high level of accuracy[8]. This research aims to create a reliable automatic detection system by utilizing classification algorithms such as Naive Bayes, which can assist in the maintenance and replacement processes of solar panels more efficiently.

Naive Bayes classification is a classification method that utilizes Bayes' probability theorem to categorize data into specific classes[9]. The uniqueness of this method lies in its "naive" or simple nature, which assumes that all features used for classification are independent of each other, even though dependencies may exist. Although this assumption seems naive, the main strength of the Naive Bayes algorithm lies in its ability to handle high-dimensional datasets, its efficiency in processing, and its resilience in facing uncertainty or diversity in the data.

The methodology of this research involves several stages. First, the collection of solar panel image data will be carried out and prepared for analysis. Next, relevant features will be extracted from the solar panel images using image processing techniques[10]. After that, the data will be divided into training and testing sets. The Naive Bayes classification model will be trained using the training set, and its performance will be evaluated using the testing set. The experimental results will be analyzed to evaluate the accuracy and performance of the algorithm in identifying damage to solar panels[11]. Various factors affecting the results, such as the type of features extracted and the size of the training data, will be discussed to understand the strengths and weaknesses of the methods used. It is hoped that the results of this research will not only provide practical contributions to the development of image-based damage identification systems for solar panel surfaces but also pave the way for further research on the application of this technology in various contexts, such as damage recognition on the surfaces of other objects in various industries[12]. By combining artificial intelligence and image analysis, this research reflects significant progress in the development of solar panel surface damage recognition technology through images.

## 2. METHOD

The methodology of this research involves several stages. First, the collection of solar panel image data will be carried out and prepared for analysis. Next, relevant features will be extracted from the solar panel images using image processing techniques. After that, the data will be divided into training and testing sets. The Naive Bayes classification model will be trained using the training set, and its performance will be evaluated using the testing set perform in Figure 1.

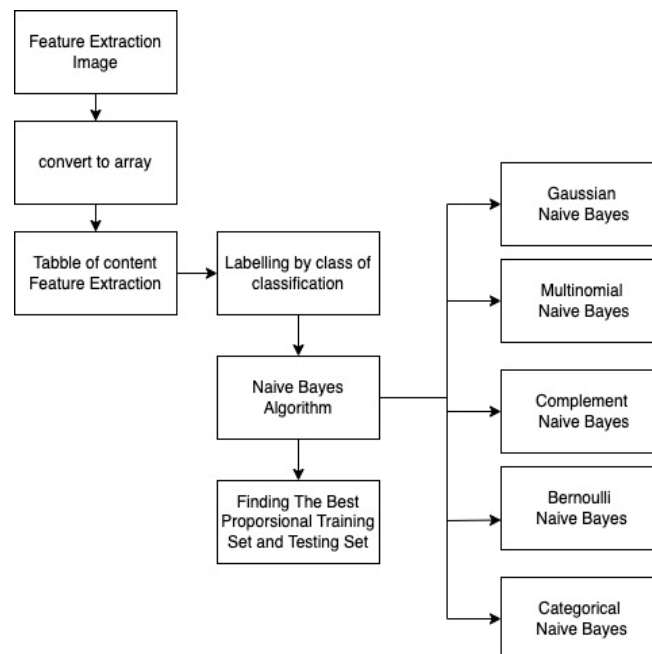


Figure 1. Classify Method with Naive Bayes

The experimental results will be analyzed to evaluate the accuracy and performance of the algorithm in identifying damage to solar panels. Various factors affecting the results, such as the type of features extracted and the size of the training data, will be discussed to understand the strengths and weaknesses of the methods used. It is hoped that the results of this research will not only provide practical contributions to the development of image-based damage identification systems for solar panel surfaces but also pave the way for further research on the application of this technology in various contexts, such as damage recognition on the surfaces of other objects in various industries. By combining artificial intelligence and image analysis, this research reflects significant progress in the development of solar panel surface damage recognition technology through images.

### 3. RESULTS AND DISCUSSION

In this section, the research results are presented based on the analysis of texture features extracted from solar panel surface images. Each statistical feature, namely Mean, Variance, Standard Deviation, Skewness, Kurtosis, and Entropy, is analyzed to assess its effectiveness in identifying types of damage, including cracks, scratches, stains, and undamaged conditions.

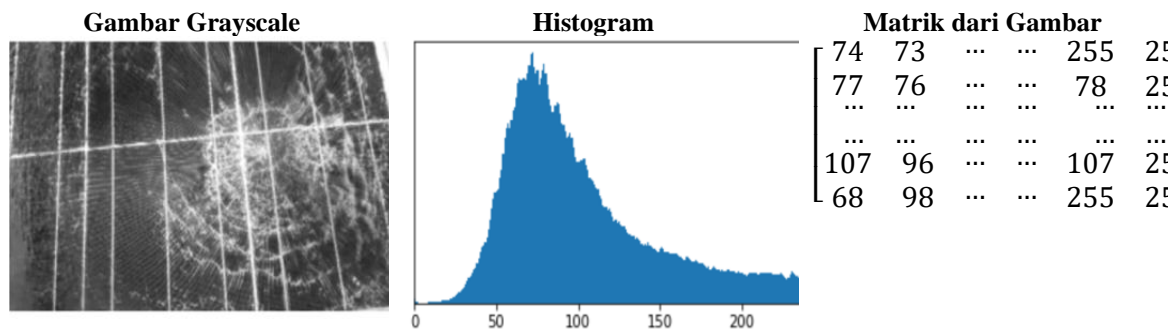


Figure 2. Covert to Matrix

Figure 2 is an example of one of the images processed using Google Colab, resulting in features that have been extracted into matrix. mean, variance, standard deviation, skewness, kurtosis, and entropy. These results were obtained from the numbers found in the histogram results. From the texture feature extraction calculations, the results for each image are as follows in figure 3.

Table 1. Result of Extract Feature

<b>Matrik dari Gambar</b>	<b>Fitur Ekstraksi</b>
$\begin{bmatrix} 74 & 73 & \dots & \dots & 255 & 255 \\ 77 & 76 & \dots & \dots & 78 & 255 \\ \dots & \dots & \dots & \dots & \dots & \dots \\ \dots & \dots & \dots & \dots & \dots & \dots \\ 107 & 96 & \dots & \dots & 107 & 255 \\ 68 & 98 & \dots & \dots & 255 & 255 \end{bmatrix}$	Mean = 102.897 Variance = 6482.891 Standard Deviation = 80.516 Skewness = 0.568 Kurtosis = -0.579 Entropy = 8.006

The combination of maximum and lowest values derived from statistical feature extraction techniques applied to photographs of the surface of solar panels is shown in Table 2. The features, encompassing metrics such as Mean, Variance, Standard Deviation, Skewness, Kurtosis, and Entropy, include vital textural characteristics crucial for the identification and classification of damage types. Through the examination of the highest and lowest values for every characteristic, this research demonstrates the variations and trends in surface textures linked to various forms of damage. These combinations function as essential inputs for the classification algorithms, facilitating a robust and precise identification process for surface faults on solar panels.

Table 2. Combination maximum and minimum feature extraction by statistical

Type	Mean		Variance		Standard Deviation		Skewness		Kurtosis		Entropy	
	Max	Min	Max	Min	Max	Min	Max	Min	Max	Min	Max	Min
Non Defect	209.179	18.088	9614.14	25.976	98.051	5.096	5.839	-7.429	261.147	-1.977	7.392	4.499
Crack	227.375	43.349	7671.45	11.151	87.586	3.339	17.181	-12.450	1326.076	-1.622	8.294	1.791
Scratch	185.814	31.373	7959.82	112.911	89.217	10.625	3.508	-7.012	205.714	-1.596	8.302	3.970
Spot	186.353	34.959	8066.54	90.637	89.814	8.402	2.907	-5.945	141.179	-1.818	7.321	4.394

The features of each defect type are examined in this chapter using a Feature Extraction technique, which is visually displayed. The data, derived from Table 3 and illustrated in Figure 3, demonstrates the statistical feature extraction technique. The x-axis displays the variables associated with the statistical traits, and the y-axis represents their corresponding frequencies. This image offers a precise comparison of feature distribution among various defect categories, emphasizing patterns and anomalies crucial for accurate categorization. Through the analysis of these graphical representations, the study acquires enhanced understanding of the unique textural characteristics that distinguish each damage category on solar panel surfaces.

Table 3. Feature extraction by statistical

	<b>Non-Defect</b>	<b>Crack</b>	<b>Scratch</b>	<b>Spot</b>
Mean	84.532	111.757	99.452	99.833
Variance	23.751	28.030	24.883	22.568
Standard Deviation	46.354	51.694	48.458	45.874
Skewness	-0.917	-0.406	-0.532	-0.607
Kurtosis	7.396	10.733	4.059	4.975
Entropy	6.135	6.487	6.115	5.923

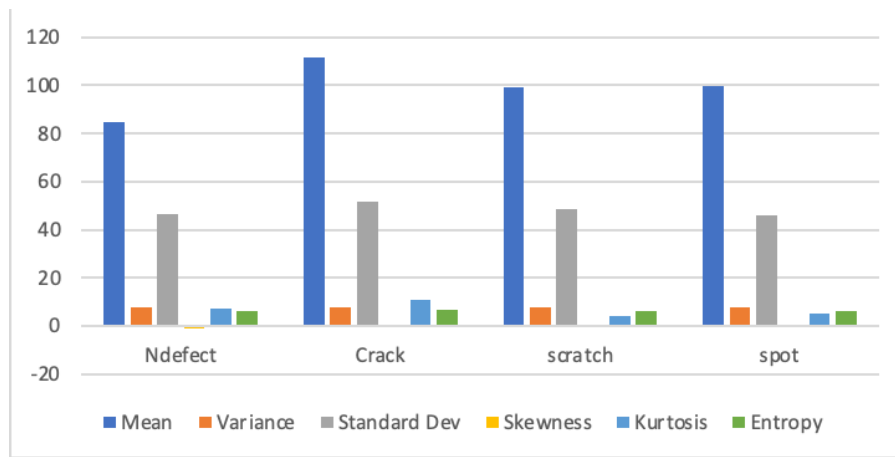


Figure 3. Illustration from Feature Extraction

The graph delineates four defect categories: non-defect, crack, scratch, and spot, alongside their corresponding statistical feature extraction values. The statistical feature extraction values include mean, variance, standard deviation, skewness, kurtosis, and entropy. The horizontal axis of the graph represents several statistical feature extraction values, while the vertical axis signifies the magnitude of these values. The graph illustrates that the statistical feature extraction values for each failure type differ significantly. The non-defect samples have relatively low values across all six statistical feature extraction metrics, but the defect samples show markedly higher values for most parameters. Among the three defect categories, the fracture samples have the highest mean, variance, and standard deviation values.

This graph facilitates understanding the differences in statistical feature extraction values across distinct fault categories. This data can be employed to develop algorithms that independently detect and classify defects based on their statistical feature extraction values. Analyzing the statistical feature extraction values of multiple samples facilitates the recognition of trends that aid in the detection and classification of defects in digital images.

Table 4. Result of classification statistical feature extraction using Bernoulli Naive Bayes

<b>Feature Extraction Method</b>	<b>Classification</b>	<b>Training : Test</b>	<b>mAP (%)</b>
Statistical	Bernoulli NB	70 : 30	28.25 %
Statistical	Bernoulli NB	75 : 25	28.30 %
Statistical	Bernoulli NB	80 : 20	27.62 %
Statistical	Bernoulli NB	85 : 15	28.00 %
Statistical	Bernoulli NB	90 : 10	29.25 %
Statistical	Bernoulli NB	95 : 05	27.50 %

To illustrate the accuracy of the approach, Table 4 presents the classification results using Bernoulli Naive Bayes utilizing Statistical FE. Accuracy is calculated by dividing the number of correctly identified photos by the total number of images in the dataset. The system is trained on a labeled dataset and subsequently evaluated on an unlabeled dataset, where the predicted class labels are compared to the actual labels. Altering the characteristics of the training and testing data can provide divergent accuracy values. The classification accuracy achieved using Statistical Feature Extraction using the Bernoulli Naive Bayes model illustrates the effectiveness of feature extraction techniques and the algorithm's performance.

Table 4 displays the performance evaluation outcomes of a classification model utilizing the statistical feature extraction technique in conjunction with the Bernoulli Naive Bayes classifier. The model was trained and assessed using diverse training-test data ratios ranging from 70:30 to 95:5. The evaluation metric utilized is mean average precision (mAP) expressed as a percentage (%). The results demonstrate that the highest mAP score of 29.25% was attained with a training-test data ratio of 90:10, while the lowest mAP score of 27.50% was noted with a training to test data ratio of 95:5. The model's performance is inadequate, underscoring the need for improvements in the feature extraction and classification methods utilized.

Table 5. Result of classification with statistical feature extraction using Gaussian Naive Bayes

Feature Extraction Method	Classification	Training : Test	mAP (%)
Statistical	Gaussian-NB	70 : 30	39.16 %
Statistical	Gaussian-NB	75 : 25	39.70 %
Statistical	Gaussian-NB	80 : 20	39.75 %
Statistical	Gaussian-NB	85 : 15	39.83 %
Statistical	Gaussian-NB	90 : 10	37.50 %
Statistical	Gaussian-NB	95 : 5	39.50 %

In subsequent trials, Gaussian Naive Bayes is employed as the classification algorithm. Table 5 displays the identical Extraction Feature, specifically Statistical, utilizing Gaussian Naive Bayes. The proportions of the training and test datasets are uniform throughout all studies. The table demonstrates that optimal performance is achieved with a training to test data ratio of 85:15, resulting in a mAP of 39.83%. Performance deteriorates with a training to test data ratio of 90:10, indicating possible overfitting from an abundance of training data. The results suggest that the statistical feature extraction technique, in conjunction with the Gaussian-NB classifier, exhibits somewhat superior effectiveness in identifying defects in solar photovoltaic modules. The Area Under the Curve (AUC) evaluates the classifier's comprehensive performance across all possible thresholds. AUC values range from 0 to 1, where 0 indicates a poor classifier, 0.5 signifies a random classifier, and 1 represents a perfect classifier. A higher AUC value indicates that the model has an improved ability to distinguish between positive and negative examples, demonstrating its superior discriminatory power. The AUC can be calculated using the formula shown in

$$AUC = \frac{Recall+Specificity}{2} \tag{1}$$

To calculate AUC, the Recall and Specificity values are required. Recall and Specificity values are added and divided by two to get the AUC value.

Table 6. Calculation of Recall

Recall = $\frac{TP}{TP + FN}$	
Recall (Crack) = $\frac{143}{143 + 172} = 0.453$	Recall (No Defect) = $\frac{154}{154 + 130} = 0.542$
Recall (Scratch) = $\frac{84}{84 + 223} = 0.273$	Recall (Spot) = $\frac{179}{179 + 115} = 0.608$
Average Recall = $\frac{R(C) + R(ND) + R(S) + R(S)}{Class} = \frac{0.453 + 0.542 + 0.273 + 0.608}{4} = 0.469$	

Recall values for each classification are shown in Table 6, which also shows the calculation of recall for the different categories (Crack, No Defect, Scratch, and Spot) and the total recall. Recall is a performance metric that quantifies the ratio of correct positive predictions to the total number of real positive cases. It is sometimes referred to as sensitivity or true positive rate.

The recall for the "Crack" class is calculated by dividing the true positives (TP) by the sum of true positives and false negatives (TP + FN). The computation results in  $143 / (143 + 172) = 0.453$ . The recall for the "No Defect" category is calculated by dividing the true positives by the sum of true positives and false negatives. The computation is 154 divided by the total of 154 and 130, yielding 0.542. The recall for the "Scratch" class is calculated as  $84 / (84 + 223) = 0.273$ . The recall for the "Spot" class is calculated as  $179 / (179 + 115) = 0.608$ . Mean Recall: Total recall is computed by summing the recall values for each class and dividing by the total number of classes. The computation is  $(0.453 + 0.542 + 0.273 + 0.608) / 4 = 0.469$ .

The recall numbers provide insights into the model's effectiveness in correctly detecting examples of each class. It evaluates the model's sensitivity in detecting positive instances for each class individually. Total recall signifies the average recall across all categories, indicating the model's overall effectiveness in identifying good instances. Recall assesses a classification model's ability to correctly identify positive instances and complements other metrics, such as precision and accuracy, in evaluating the model's overall effectiveness. Specificity is a performance metric used in binary classification to evaluate a model's ability to identify negative data. The computation represents the ratio of true negatives (TN) to the sum of true negatives (TN) and false positives (FP).

Table 7. Measurement of specificity

<b>Specificity = <math>\frac{TN}{TN + FP}</math></b>	
<b>Specificity (Crack) = <math>\frac{738}{738 + 147} = 0.833</math></b>	<b>Specificity (No Defect) = <math>\frac{865}{865 + 51} = 0.944</math></b>
<b>Specificity (Scratch) = <math>\frac{703}{703 + 149} = 0.825</math></b>	<b>Specificity (Spot) = <math>\frac{613}{613 + 293} = 0.676</math></b>
<b>Total Specificity = <math>\frac{S(ND) + S(C) + S(S) + S(S)}{Class} = \frac{0.833 + 0.944 + 0.825 + 0.676}{4} = 0.819</math></b>	

The specificity values for the several classes (Crack, No Defect, Scratch, and Spot) as well as the total specificity are calculated and shown in Table 7. Specificity, or the real negative rate, measures the proportion of accurate negative predictions relative to the total number of actual negative cases. The specificity for the "Crack" class is calculated by dividing the true negatives (TN) by the sum of true negatives and false positives (TN + FP). The computation is 738 divided by the total of 738 and 147, yielding 0.833. The specificity for the "No Defect" class is calculated by dividing the number of true negatives by the sum of true negatives and false positives. The computation is 865 divided by the total of 865 and 51, yielding 0.944. The specificity for the "Scratch" class is calculated as  $703 / (703 + 149) = 0.825$ . The specificity for the "Spot" class is calculated as  $613 / (613 + 293) = 0.676$ . The average specificity is determined by summing the specificity values for each class and dividing by the total number of classes. The computation results in  $(0.833 + 0.944 + 0.825 + 0.676) / 4 = 0.819$ .

The specificity values reflect the model's ability to correctly identify negative occurrences for each class. It evaluates the model's ability to avert false positive predictions. Total specificity represents the average specificity across all classes, indicating the model's overall effectiveness in identifying negative instances. The Recall and Specificity values have been obtained, enabling the computation of the Area Under the Curve by inserting the Recall and Specificity values into the AUC formula in (2.37). The following calculation relates to the AUC value:

$$AUC = \frac{0.469 + 0.819}{2} = 0.644 = 64.4 \%$$

The calculation shows how the Area Under the Curve (AUC) value was determined. The AUC is a widely used metric for evaluating the effectiveness of a classification model. It evaluates the model's ability to distinguish between positive and negative cases across all possible classification thresholds.

The Recall value is determined by summing the recall values for each class (Crack, No Defect, Scratch, Spot) and dividing by the total number of classes. The computation is  $(0.453 + 0.542 + 0.273 + 0.608) / 4 = 0.469$ . The specificity value is calculated by summing the specificity values for each class and dividing by the total number of classes. The computation results in  $(0.833 + 0.944 + 0.825 + 0.676) / 4 = 0.819$ . The total AUC is obtained by averaging the AUC values calculated for recall and specificity. The computation is  $(0.469 + 0.819) / 2 = 0.644$ .

The AUC value ranges from 0 to 1, with a higher value indicating enhanced performance. An AUC of 0.5 denotes a model with no discriminatory ability, whereas an AUC of 1 represents a perfect model. The

model attained an AUC value of 0.644. It has been demonstrated that it can precisely differentiate 64.4% of the total actual occurrences.

#### 4. CONCLUSION

This research explores the use of statistical feature extraction techniques to identify and classify various types of damage on solar panels through digital images. Two classification algorithms, namely Bernoulli Naive Bayes (BNB) and Gaussian Naive Bayes (GNB), were used to evaluate the effectiveness of this approach. The analysis results show that GNB performs better than BNB, with the highest mean average precision (mAP) of 39.83% at a training and testing data ratio of 85:15. In contrast, BNB achieved the highest mAP of 29.25% at a 90:10 ratio, but its overall performance was less optimal. The decline in performance at several data ratios indicates the need for improvements in feature extraction techniques and classification algorithms to address the model's limitations.

Additionally, metrics such as recall, specificity, and area under the curve (AUC) are used to evaluate the model's performance comprehensively. The average recall value of 0.469 indicates that the model still has weaknesses in detecting positive cases, while the average specificity value of 0.819 shows a fairly good ability to avoid false positive predictions. An AUC of 0.644 indicates that the model has a moderate ability to distinguish between positive and negative cases. Overall, this study shows that the combination of statistical feature extraction techniques and the Naive Bayes algorithm can be used for classifying solar panel damage, but further development is needed to improve its accuracy and effectiveness.

#### REFERENCES

- [1] Neha and R. Joon, "Renewable Energy Sources: A Review," *J Phys Conf Ser*, vol. 1979, p. 012023, Aug. 2021, doi: 10.1088/1742-6596/1979/1/012023.
- [2] M. RASLAN and E. Çam, "Fault Detection and Diagnosis Technic Using Electrical Characteristics of a PV Module and Machine Learning Classifier," *Uluslararası Muhendislik Arastirma ve Gelistirme Dergisi*, 2020, doi: 10.29137/umagd.843768.
- [3] Q. Luo *et al.*, "Surface defect classification for hot-rolled steel strips by selectively dominant local binary patterns," *IEEE Access*, vol. 7, pp. 1–10, 2019, doi: 10.1109/ACCESS.2019.2898215.
- [4] N. Wiliani, A. Sani, and A. T. Andyanto, "Klasifikasi Kerusakan Dengan Jaringan Syaraf Backpropagation Pada Permukaan Solar Panel," *JITK (Jurnal Ilmu Pengetahuan dan Teknologi Komputer)*, vol. 5, no. 1, pp. 89–94, 2019, doi: 10.33480/jitk.v5i1.662.
- [5] J. Cervantes, F. Garcia-Lamont, L. Rodríguez-Mazahua, and A. Lopez, "A comprehensive survey on support vector machine classification: Applications, challenges and trends," *Neurocomputing*, vol. 408, pp. 189–215, 2020.
- [6] N. Wiliani, A. Sani, and S. Ramli, "Statistical ICharacteristics For Identification Defect of Solar Panel with Naive Statistical Characteristics For Identification Defect of Solar Panel with Naive Bayes," no. December, 2019, doi: 10.31227/osf.io/uyfne.
- [7] S. Umar, M. U. Nawaz, and M. S. Qureshi, "Deep Learning Approaches for Crack Detection in Solar PV Panels," *International Journal of Advanced Engineering Technologies and Innovations*, vol. 1, no. 3, pp. 50–72, 2024.
- [8] A. Sani, T. Abdul Rahman, A. Subiyakto, and N. Wiliani, "Combining Statistical and Interpretative Analyses for Testing Readiness and IT Adoption Questionnaire," 2019, doi: 10.4108/eai.27-4-2019.2286808.
- [9] A. Rebinth and M. Kumar S, *Image Processing Using Naive Bayes Classifier*. 2020.
- [10] S. Deitsch *et al.*, "Automatic classification of defective photovoltaic module cells in electroluminescence images," *Solar Energy*, vol. 185, pp. 455–468, Jun. 2019, doi: 10.1016/j.solener.2019.02.067.
- [11] P. Dinesh, A. S. Vickram, and P. Kalyanasundaram, "Medical image prediction for diagnosis of breast cancer disease comparing the machine learning algorithms: SVM, KNN, logistic regression, random forest and decision tree to measure accuracy," in *AIP Conference Proceedings*, AIP Publishing, 2024.
- [12] P. .R, S. Sathiamoorthy, and M. Kaliyamoorthi, "A Review of Image Classification Approaches and Techniques," Mar. 2020, doi: 10.23883/IJRTER.2017.3033.XTS7Z.